The computations for the error of the center of gravity are quite similar. With the same assumptions about the segmentation process, an unbiased estimate of the center of gravity is given by

$$\boldsymbol{x}_g = \frac{1}{N}\left(\sum_{n=1}^{N-N_b} \boldsymbol{x}_n + \frac{1}{2}\sum_{n'=1}^{N_b} \boldsymbol{x}_{n'}\right) \tag{8.18}$$

Again the border pixels are counted only half. As the first part of the estimate with the nonborder pixels is exact, errors are caused only by the variation in the area of the border pixels. Therefore the variance of the estimate for each component of the center of gravity is given by

$$\sigma_g^2 = \frac{N_b}{4N^2}\sigma^2 \tag{8.19}$$

where σ is again the variance in the position of the fractional cells at the border of the object. Thus the standard deviation of the center of gravity for a compact object with the diameter of D pixels is

$$\sigma_g \approx \frac{0.3}{D^{3/2}} \quad \text{if } D \gg 1 \tag{8.20}$$

Thus the standard deviation for the center of gravity of an object with 10 pixel diameter is only about 0.01 pixel. For a volumetric object with a diameter of D pixel, the standard deviation becomes

$$\sigma_{gv} \approx \frac{0.45}{D^2} \quad \text{if } D \gg 1 \tag{8.21}$$

This result clearly shows that the position of objects and all related geometrical quantities such as the distances can be performed even with binary images (segmented objects) well into the range of 1/100 pixel. It is interesting that the relative errors for the area and volume estimates of Eqs. (8.16) and (8.17) are equal to the standard deviation of the center of gravity Equations (8.20) and (8.21). Note that only the *statistical error* has been discussed. A bias in the segmentation might easily result in much higher systematic errors.

8.4 Relation between continuous and discrete signals

A continuous function $g(\boldsymbol{q})$ is a useful mathematical description of a signal as discussed in Section 8.2. Real-world signals, however, can only be represented and processed as discrete or digital signals. Therefore a detailed knowledge of the relation between these two types of signals is required. It is not only necessary to understand the whole chain of the image-formation process from a continuous spatial radiance distribution to a digital image but also to perform subpixel-accurate image

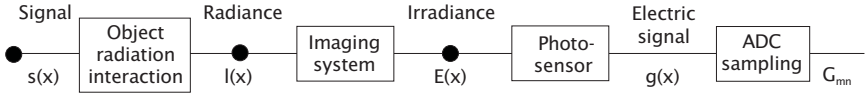

Figure 8.7: *Steps from a continuous to a discrete signal.*

interpolation (Section 9.6) and warping of images [CVA2, Chapter 9] as it is, for example, required for multiscale image operations [CVA2, Chapter 14].

The chain of processes that lead from the "true" signal to the digital signal include all the steps of the image-formation process as illustrated in Fig. 8.7. First, the signal of interest $s(\boldsymbol{x})$, such as reflectivity, temperature, etc., of an object, is somehow related to the radiance $L(\boldsymbol{x})$ emitted by the object in a generally nonlinear function (Section 2.5). In some cases this relation is linear (e. g., reflectivity), in others it is highly nonlinear (e. g., temperature). Often other parameters that are not controlled or not even known influence the signal as well. As an example, the radiance of an object is the product of its reflectivity and the irradiance. Moreover, the radiance of the beam from the object to the camera may be attenuated by absorption or scattering of radiation (Section 2.5.3). Thus the radiance of the object may vary with many other unknown parameters until it finally reaches the radiation-collecting system (optics).

The optical system generates an irradiance $E(\boldsymbol{x})$ at the image plane that is proportional to the object radiance (Chapter 4). There is, however, not a point-to-point correspondence. Because of the limited resolution of the optical systems due to physical limitation (e. g., diffraction) or imperfections of the optical systems (various aberrations; Section 3.5). This blurring of the signal is known as the *point spread function* (*PSF*) of the optical system and described in the Fourier domain by the *optical transfer function*. The nonzero area of the individual sensor elements of the sensor array (or the scanning mechanism) results in a further spatial and temporal blurring of the irradiance at the image plane.

The conversion to electrical signal U adds noise and possibly further nonlinearities to the signal $g(\boldsymbol{x}, t)$ that is finally measured. In a last step, the analog electrical signal is converted by an *analog-to-digital converter* (*ADC*) into digital numbers. The basic relation between continuous and digital signals is established by the sampling theorem. It describes the effects of spatial and temporal sampling on continuous signals and thus also tells us how to reconstruct a continuous signal from its samples.

The image-formation process itself thus includes two essential steps. First, the whole image-formation process blurs the signal. Second, the

continuous signal at the image plane is sampled. Although both processes often occur together, they can be separated for an easier mathematical treatment.

8.4.1 Image formation

If we denote the undistorted original signal projected onto the image plane by $g'(\boldsymbol{x},t)$, then the signal $g(\boldsymbol{x},t)$ modified by the image-formation process is given by

$$g(\boldsymbol{x},t) = \int_{-\infty}^{\infty} g'(\boldsymbol{x}',t')h(\boldsymbol{x},\boldsymbol{x}',t,t')\,\mathrm{d}^2x'\,\mathrm{d}t' \tag{8.22}$$

The function h is the PSF. The signal $g'(\boldsymbol{x},t)$ can be considered as the image that would be obtained by a perfect system, that is, an optical system whose PSF is a δ-distribution. Equation (8.22) indicates that the signal at the point $[\boldsymbol{x},t]^T$ in space and time is composed of the radiance of a whole range of points $[\boldsymbol{x}',t']^T$ nearby, which linearly add up weighted with the signal h at $[\boldsymbol{x}',t']^T$. The integral can significantly be simplified if the point-spread function is the same at all points (*homogeneous system* or *shift-invariant system*). Then the point-spread function h depends only on the distance of $[\boldsymbol{x}',t']^T$ to $[\boldsymbol{x},t]^T$ and the integral in Eq. (8.22) reduces to the *convolution* integral

$$g(\boldsymbol{x},t) = \int_{-\infty}^{\infty} g'(\boldsymbol{x}',t')h(\boldsymbol{x}-\boldsymbol{x}',t-t')\,\mathrm{d}^2x'\,\mathrm{d}t' = (g' * h)(\boldsymbol{x},t) \tag{8.23}$$

For most optical systems the PSF is not strictly shift-invariant because the degree of blurring is increasing with the distance from the optical axis (Chapter 3). However, as long as the variation is continuous and does not change significantly over the width of the PSF, the convolution integral in Eq. (8.23) still describes the image formation correctly. The PSF and the system transfer function just become weakly dependent on $\boldsymbol{x}$.

8.4.2 Sampling theorem

Sampling means that all information is lost except at the grid points. Mathematically, this constitutes a multiplication of the continuous function with a function that is zero everywhere except for the grid points. This operation can be performed by multiplying the image function $g(\boldsymbol{x})$ with the sum of δ distributions located at all lattice vectors $\boldsymbol{r}_{m,n}$ as in Eq. (8.7). This function is called the two-dimensional δ comb, or

"nail-board function." Then sampling can be expressed as

$$g_s(\boldsymbol{x}) = g(\boldsymbol{x}) \sum_{m=-\infty}^{m=\infty} \sum_{n=-\infty}^{n=\infty} \delta(\boldsymbol{x} - \boldsymbol{r}_{m,n}) \tag{8.24}$$

This equation is only valid as long as the elementary cell of the lattice contains only one point. This is the case for the square and hexagonal grids (Fig. 8.2b and c). The elementary cell of the triangular grid, however, includes two points (Fig. 8.2a). Thus for general regular lattices, p points per elementary cell must be considered. In this case, a sum of P δ combs must be considered, each shifted by the offsets $\boldsymbol{s}_p$ of the points of the elementary cells:

$$g_s(\boldsymbol{x}) = g(\boldsymbol{x}) \sum_{p=1}^{P} \sum_{m=-\infty}^{\infty} \sum_{n=-\infty}^{\infty} \delta(\boldsymbol{x} - \boldsymbol{r}_{m,n} - \boldsymbol{s}_p) \tag{8.25}$$

It is easy to extend this equation for sampling into higher-dimensional spaces and into the time domain:

$$g_s(\boldsymbol{x}) = g(\boldsymbol{x}) \sum_{p} \sum_{\boldsymbol{n}} \delta(\boldsymbol{x} - \boldsymbol{r}_{\boldsymbol{n}} - \boldsymbol{s}_p) \tag{8.26}$$

In this equation, the summation ranges have been omitted. One of the coordinates of the D-dimensional space and thus the vector $\boldsymbol{x}$ and the lattice vector $\boldsymbol{r}_{\boldsymbol{n}}$

$$\boldsymbol{r}_{\boldsymbol{n}} = [n_1\boldsymbol{b}_1, n_2\boldsymbol{b}_2, \ldots, n_D\boldsymbol{b}_D]^T \quad \text{with} \quad n_d \in \mathbb{Z} \tag{8.27}$$

is the time coordinate. The set of fundamental translation vectors $\{\boldsymbol{b}_1, \boldsymbol{b}_2, \ldots, \boldsymbol{b}_D\}$ form a not necessarily orthogonal base spanning the D-dimensional space.

The sampling theorem directly results from the Fourier transform of Eq. (8.26). In this equation the continuous signal $g(\boldsymbol{x})$ is multiplied by the sum of delta distributions. According to the convolution theorem of the Fourier transform (Section 8.6), this results in a convolution of the Fourier transforms of the signal and the sum of delta combs in Fourier space. The Fourier transform of a delta comb is again a delta comb (see Table 8.5). As the convolution of a signal with a delta distribution simply replicates the function value at the zero point of the delta functions, the Fourier transform of the sampled signal is simply a sum of shifted copies of the Fourier transform of the signal:

$$\hat{g}_s(\boldsymbol{k}, \nu) = \sum_{p} \sum_{\boldsymbol{v}} \hat{g}(\boldsymbol{k} - \hat{\boldsymbol{r}}_{\boldsymbol{v}}) \exp\left(-2\pi \mathrm{i} \boldsymbol{k}^T \boldsymbol{s}_p\right) \tag{8.28}$$

The phase factor $\exp(-2\pi \mathrm{i} \boldsymbol{k}^T \boldsymbol{s}_p)$ results from the shift of the points in the elementary cell by $\boldsymbol{s}_p$ according to the shift theorem of the Fourier

transform (see Table 8.4). The vectors $\hat{\boldsymbol{r}}_{\boldsymbol{v}}$

$$\hat{\boldsymbol{r}}_{\boldsymbol{v}} = v_1\hat{\boldsymbol{b}}_1 + v_2\hat{\boldsymbol{b}}_2 + \ldots + v_D\hat{\boldsymbol{b}}_D \quad \text{with} \quad v_d \in \mathbb{Z} \tag{8.29}$$

are the points of the so-called *reciprocal lattice*. The fundamental translation vectors in the space and Fourier domain are related to each other by

$$\boldsymbol{b}_d^T\hat{\boldsymbol{b}}_{d'} = \delta_{d-d'} \tag{8.30}$$

This basically means that the fundamental translation vector in the Fourier domain is perpendicular to all translation vectors in the spatial domain except for the corresponding one. Furthermore, the distances are reciprocally related to each other. In 3-D space, the fundamental translations of the reciprocial lattice can therefore be computed by

$$\hat{\boldsymbol{b}}_d = \frac{\boldsymbol{b}_{d+1} \times \boldsymbol{b}_{d+2}}{\boldsymbol{b}_1^T(\boldsymbol{b}_2 \times \boldsymbol{b}_3)} \tag{8.31}$$

The indices in the preceding equation are computed modulo 3, $\boldsymbol{b}_1^T(\boldsymbol{b}_2 \times \boldsymbol{b}_3)$ is the volume of the primitive elementary cell in the spatial domain. All these equations are familiar to solid state physicists or cristallographers [3]. Mathematicians know the lattice in the Fourier domain as the *dual base* or *reciprocal base* of a vector space spanned by a nonorthogonal base. For an orthogonal base, all vectors of the dual base show into the same direction as the corresponding vectors and the magnitude is given by $\left|\hat{\boldsymbol{b}}_d\right| = 1/|\boldsymbol{b}_d|$. Then often the length of the base vectors is denoted by Δx_d, and the length of the reciprocal vectors by $\Delta k_d = 1/\Delta x_d$. Thus an orthonormal base is dual to itself.

For further illustration, Fig. 8.8 shows the lattices in both domains for a triangular, square, and hexagonal grid. The figure also includes the primitive cell known as the *Wigner-Seitz cell* (Section 8.3.1 and Fig. 8.3) and first *Brillouin zone* in the spatial and Fourier domain, respectively.

Now we can formulate the condition where we get no distortion of the signal by sampling, known as the *sampling theorem*. If the image spectrum $\hat{g}(\boldsymbol{k})$ contains such high wave numbers that parts of it overlap with the periodically repeated copies, we cannot distinguish whether the spectral amplitudes come from the original spectrum at the center or from one of the copies. In other words, a low wave number can be an alias of a high wave number and assume an incorrect amplitude of the corresponding wave number. In order to obtain no distortions, we must avoid overlapping. A safe condition to avoid overlapping is as follows: the spectrum must be zero outside of the primitive cell of the reciprocal lattice, that is, the first Brillouin zone.

On a rectangular grid, this results in the simple condition that the maximum wave number (or frequency) at which the image spectrum

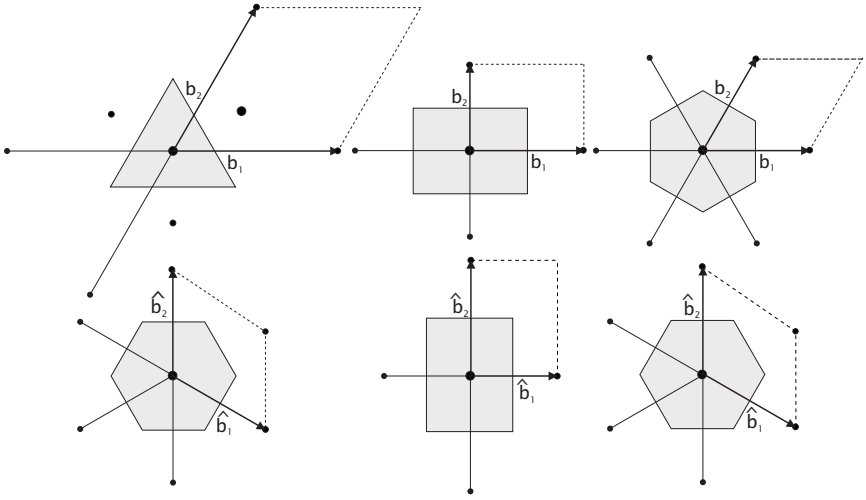

Figure 8.8: *Lattices with the fundamental translation vectors and primitive cell in the spatial and Fourier domain for a triangular (left), square (middle), and hexagonal (right) 2-D lattice.*

is not equal to zero must be restricted to less than half of the grid constants of the reciprocal grid. Therefore the sampling theorem is as follows:

Theorem 8.1 (Sampling Theorem) *If the spectrum $\hat{g}(\boldsymbol{k})$ of a continuous function $g(\boldsymbol{x})$ is* band-limited, *that is,*

$$\hat{g}(\boldsymbol{k}) = 0 \quad \forall\, |k_d| \geq \Delta k_d/2 \tag{8.32}$$

then it can be reconstructed exactly from samples with a distance

$$\Delta x_d = 1/\Delta k_d \tag{8.33}$$

In other words, we will obtain a periodic structure correctly only if we take at least two samples per wavelength (or period). The maximum wave number that can be sampled without errors is called the *Nyquist* or *limiting* wave number (or frequency). In the following, we will often use dimensionless wave numbers (frequencies), which are scaled to the limiting wave number (frequency). We denote this scaling with a tilde:

$$\tilde{k}_d = \frac{k_d}{\Delta k_d/2} = 2k_d\Delta x_d \quad \text{and} \quad \tilde{\nu} = \frac{\nu}{\Delta\nu/2} = 2\nu\Delta T \tag{8.34}$$

In this scaling all the components of the wave number $\tilde{k}_d$ fall into the interval $]-1, 1[$.

8.4.3 Aliasing

If the conditions of the sampling theorem are not met, it is not only impossible to reconstruct the original signal exactly but also distortions are introduced into the signal. This effect is known in signal theory as *aliasing* or in imaging as the *Moiré effect*.

The basic problem with aliasing is that the band limitation introduced by the blurring of the image formation and the nonzero area of the sensor is generally not sufficient to avoid aliasing. This is illustrated in the following example with an "ideal" sensor.

Example 8.1: Standard sampling

An "ideal" imaging sensor will have a nonblurring optics (the PSF is the delta distribution) and a sensor array that has a 100% fill factor, that is, the sensor elements show a constant sensitivity over the whole area without gaps inbetween. The PSF of such an imaging sensor is a box function with the width Δx of the sensor elements and the transfer function (TF) is a sinc function:

$$\begin{aligned} &\text{PSF} && \frac{1}{\Delta x_1}\Pi(x_1/\Delta x_1)\frac{1}{\Delta x_2}\Pi(x_2/\Delta x_2) \\ &\text{TF} && \frac{\sin(\pi k_1 \Delta x_1)}{\pi k_1 \Delta x_1}\frac{\sin(\pi k_2 \Delta x_2)}{\pi k_2 \Delta x_2} \end{aligned} \tag{8.35}$$

The sinc function has its first zero crossings when the argument is $\pm\pi$. This is when $k_d = \pm\Delta x_d$ or at twice the Nyquist wave number, see Eq. (8.34). At the Nyquist wave number the value of the transfer function is still $1/\sqrt{2}$. Thus standard sampling is not sufficient to avoid aliasing. The only safe way to avoid aliasing is to ensure that the imaged objects do not contain wave numbers and frequencies beyond the Nyquist limit.

8.4.4 Reconstruction from samples

The sampling theorem ensures the conditions under which we can reconstruct a continuous function from sampled points, but we still do not know how to perform the reconstruction of the continuous image from its samples, that is, the inverse operation to sampling.

Reconstruction is performed by a suitable *interpolation* of the sampled points. Again we use the most general case: a nonorthogonal primitive cell with P points. Generally, the interpolated points $g_r(\boldsymbol{x})$ are calculated from the values sampled at $\boldsymbol{r_n}+\boldsymbol{s}_p$ weighted with suitable factors that depend on the distance from the interpolated point:

$$g_r(\boldsymbol{x}) = \sum_p \sum_{\boldsymbol{n}} g_s(\boldsymbol{r_n} + \boldsymbol{s}_p) h(\boldsymbol{x} - \boldsymbol{r_n} - \boldsymbol{s}_p) \tag{8.36}$$

Using the integral property of the δ distributions, we can substitute the sampled points on the right-hand side by the continuous values

and then interchange summation and integration:

$$\begin{aligned} g_r(\boldsymbol{x}) &= \sum_p \sum_{\boldsymbol{n}} \int_{-\infty}^{\infty} g(\boldsymbol{x}')h(\boldsymbol{x}-\boldsymbol{x}')\delta(\boldsymbol{r}_{\boldsymbol{n}}+\boldsymbol{s}_p-\boldsymbol{x}')\,\mathrm{d}^D x' \\ &= \int_{-\infty}^{\infty} h(\boldsymbol{x}-\boldsymbol{x}') \sum_p \sum_{\boldsymbol{n}} \delta(\boldsymbol{r}_{\boldsymbol{n}}+\boldsymbol{s}_p-\boldsymbol{x}')g(\boldsymbol{x}')\,\mathrm{d}^D x' \end{aligned}$$

The latter integral is a convolution of the weighting function h with a function that is the sum of the product of the image function g with shifted δ combs. In Fourier space, convolution is replaced by complex multiplication and vice versa. If we further consider the shift theorem and that the Fourier transform of a δ comb is again a δ comb, we finally obtain

$$\hat{g}_r(\boldsymbol{k}) = \hat{h}(\boldsymbol{k}) \sum_p \sum_{\boldsymbol{v}} \hat{g}(\boldsymbol{k}-\hat{\boldsymbol{r}}_{\boldsymbol{v}}) \exp\left(-2\pi \mathrm{i} \boldsymbol{k}^T \boldsymbol{s}_p\right) \tag{8.37}$$

The interpolated function can only be equal to the original image if the periodically repeated image spectra are not overlapping. This is nothing new; it is exactly what the sampling theorem states. The interpolated image function is only equal to the original image function if the weighting function is one within the first Brillouin zone and zero outside, eliminating all replicated spectra and leaving the original band-limited spectrum unchanged. On a D-dimensional orthogonal lattice Eq. (8.37) becomes

$$\hat{g}_r(\boldsymbol{k}) = \hat{g}(\boldsymbol{k}) \prod_{d=1}^{D} \Pi(k_d \Delta x_d) \tag{8.38}$$

and the ideal interpolation function h is the sinc function

$$h(\boldsymbol{x}) = \prod_{d=1}^{D} \frac{\sin(\pi x_d/\Delta x_d)}{\pi x_d/\Delta x_d} \tag{8.39}$$

Unfortunately, this function decreases only with $1/x$ towards zero. Therefore, a correct interpolation requires a large image area; mathematically, it must be infinitely large. This condition can be weakened if we "overfill" the sampling theorem, that is, ensure that $\hat{g}(\boldsymbol{k})$ is already zero before we reach the Nyquist limit. According to Eq. (8.37), we can then choose $\hat{h}(\boldsymbol{k})$ arbitrarily in the region where $\hat{g}$ vanishes. We can use this freedom to construct an interpolation function that decreases more quickly in the spatial domain, that is, has a minimum-length interpolation mask. We can also start from a given interpolation formula. Then the deviation of its Fourier transform from a box function tells us to what extent structures will be distorted as a function of the wave number. Suitable interpolation functions will be discussed in detail in Section 9.6.